5

Shock-Induced Solid–Solid Reactions and Detonations

Yu.A. Gordopolov, S.S. Batsanov, and V.S. Trofimov

5.1 Introduction

In this chapter, we consider the theoretical and practical aspects of shock wave processes in condensed media, including solid–solid detonations (SSDs), i.e., conversion of solid-phase reactants to solid-phase products [1]. Numerous experimental data imply that shock processing may be used to induce very fast chemical reactions in compacted reactive powder mixtures.

It is known [2] that a shock wave process is a kind of motion in a continuous medium which is accompanied by propagation of special waves (shocks) at a hypersound velocity. A shock (sudden change) represents a thin, relatively stable zone within which elementary volumes of matter spasmodically change their velocity and density. Depending on the properties of the medium, either compression or rarefaction shocks can be formed. Since rarefaction shocks are encountered infrequently, in further discussion we will deal only with compression shocks.

Within the shock, the medium may undergo various physicochemical transformations (chemical reaction, phase transition, collapse of pores, etc.). Shocks without transformations and shocks in chemically inert porous media are normally termed "shock waves." The shocks accompanied by physicochemical transformations are termed either "shock waves" or "detonation waves," depending on the type of transformation. The difference between shock waves and detonation waves will be discussed later. Now let us only note that a leading shock in a self-propagating shock wave process in condensed explosives or reactive gaseous mixtures can be classified as a detonation wave. Concerning other shock wave processes, the difference between shock and detonation waves is a subject of controversy and argument.

The width of shocks without transformation of matter is comparable to the free path of molecules in gases or to intermolecular distance in condensed matter [2]. As a mathematical image of such a shock, the notion of a traveling finite discontinuity surface can be used. The width of a shock accompanied by transformations of matter is greater by several orders of magnitude. For

F. Zhang (ed.), *Shock Wave Science and Technology Reference Library: Heterogeneous Detonation*, DOI: 10.1007/978-3-540-88447-7_5,

instance, in powder mixtures the shock width is comparable to the particle size. Nevertheless, in some cases the shock with transformation can also be modeled as a surface of finite discontinuity.

It is believed that a self-sustained shock wave process (detonation) may develop only in condensed explosives or reactive gaseous mixtures where the reaction is accompanied by vigorous gas evolution. The possibility of detonation in systems that react without evolution of gases (so-called gas-free detonation) has been predicted theoretically [3], and a quantitative thermodynamic criterion for this to occur in any condensed media was suggested in [3] and then specified in [4] (see Sect. 5.4.4).

5.2 Shock-Induced Solid–Solid Reactions

5.2.1 Experimental Observations

For the first time, the occurrence of shock-induced solid–solid reactions (SSRs) was detected in experiments with recovery fixtures [5]. A key point here is the duration of the SSR. When the reaction is accomplished in microseconds (i.e., within the high-pressure zone), one can expect nontrivial results. Otherwise, the reaction will proceed upon unloading as a result of heating. In this case, we deal with conventional thermal reactions. The reaction time can be measured by the kinetic method suggested in [6]. But since such shock wave experiments are difficult to carry out even in well-equipped laboratories, we have to seek other indirect ways to resolve the problem.

The reaction time can be measured directly or indirectly, by the presence/absence of high-pressure phases in synthesized products. Here we will analyze the available experimental data with special emphasis on the mechanism of ultrafast transport phenomena taking place during SSRs within the shock wave.

5.2.2 Temperature Measurements

Our temperature measurements [7–11] for the Sn–S system allowed us to gradually decrease the inertia of experiments from 10^{-1} s to below 10^{-4} s through the use of thinner and thinner wires and foils. These measurements were conducted in recovery ampoules rigidly fixed to a massive steel plate.

Shock experiments were carried out under similar conditions [standard steel ampoule, high explosive (HE) RDX, porosity of samples about 30%] with powders of Sn, S, SnS (nonreactive powders), and Sn–S (reactive mixture). The residual temperature (in 10^{-1} s after explosion) was found to be 110, 120, 130, and 1,110°C, respectively.

For the complete conversion Sn + S → SnS, the product temperature is expected to be 1,960°C ($\Delta H_r = 110.2\,\mathrm{kJ\,mol^{-1}}$, $c_p = 49.3\,\mathrm{J\,kmol^{-1}}$). This implies that the degree of conversion was around 0.56 (obtained as a ratio of the

measured temperature of 1,110–1,960°C, corresponding to 100% conversion). The recovered sample data showed that the reaction occurred largely within the axial region of the cylinder (in the so-called Mach stem). The conversion degree and product composition (SnS or SnS_2) were found to depend on the particle size of the original powder, which is indicative of SSRs. The above conclusion was also supported by calorimetric data.

Further improvement in the time resolution of temperature measurements was achieved by using optical pyrometry. For the systems Al–Fe_2O_3 [12], Ni–Al [13, 14], Sn–S [15], and Sn–Te [16], taken as examples, the reaction was completed within 10^{-7} s. In 10 ns, the temperature of the Sn–S mixture was found to reach 1,300°C [15]. The bell-shaped dependence of ΔT on p (curve 3 in Fig. 5.1) implies that the reaction may proceed only within a limited range of p: with increasing p, the formation of SnS (accompanied by an increase in v) is promoted, while ΔH_r tends to decrease [17].

The temperature profile for shock-induced SSRs of Mg, Al, and Ti with S was measured in real-time experiments [18, 19]. In the above-mentioned mixtures, SSRs proceed within 50 ns behind the shock front at a conversion

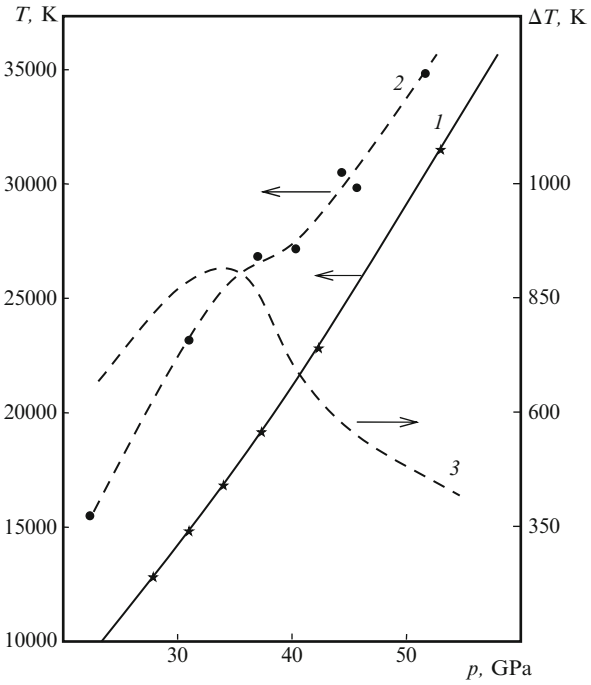

Fig. 5.1. The pressure dependence of T and ΔT for the Sn + S mixture. *1* inert mixture (T_1), *2* reactive mixture (T_2), and *3* $\Delta T = T_1 - T_2$ [15]

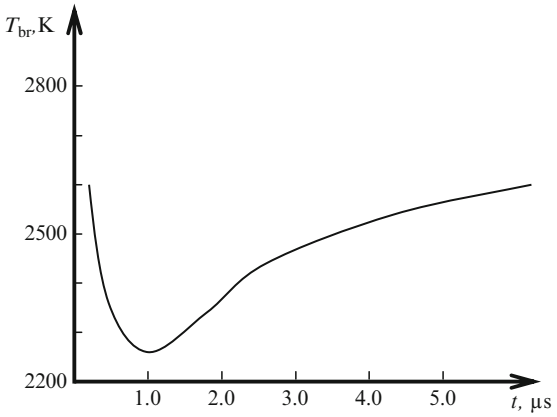

Fig. 5.2. Brightness temperature T_{br} versus time t for the shock-induced solid–solid reaction of Mg with S [18, 19]

degree of 0.2 for Mg–S and 0.5 for Al–S. Optical measurements with the Al–S system have shown that the reaction kinetics depends on the size of the reactive particles, which is also indicative of SSRs.

In the case of the Mg–S system loaded with a cast TNT–RDX explosive [18, 19], the primary peak was found to be followed by a subsequent gradual rise in temperature caused by the reaction taking place after the drop of pressure (Fig. 5.2). Such behavior is similar to that in the recovery ampoule.

5.2.3 Kinematic Measurements

A well-known example of ultrafast reactions is the detonation of HEs: this involves an intramolecular process which is not controlled by diffusion. It has been established experimentally that shock-induced solid–gas reactions can be accomplished in microseconds [20, 21]. A similar situation was observed under shock compression of the $Pb(NO_3)_2$–Al system. The curves of shock compression for $Pb(NO_3)_2$ and $Pb(NO_3)_2 + 5\%$ Al systems [22] show that, for $p > 3.5$ GPa, the reaction is accompanied by an increase in p.

The diffusion rate in solids is known to be exceedingly slow: 0.1–1.0 mm s^{-1} under normal conditions and even slower under high pressure [2]. For this reason, an ultrafast SSR within the shock appears unlikely.

In view of this, the observed [23] shift of the curve of shock compression for the Sn–S mixture for $p \geq 15$ GPa toward greater v and/or p seemed unexpected. The kinematic measurements [23] gave a conversion degree of 0.27 ± 0.1 in 0.5 μs after explosion, which agreed qualitatively with temperature measurement data (see Sect. 5.2.2). Later, the kinematic measurement data confirmed the occurrence of SSRs in the Sn–Te system for $p \geq 45$ GPa [16] and in the Ti–C mixture for $p \geq 7.5$ GPa [24] (Fig. 5.3).

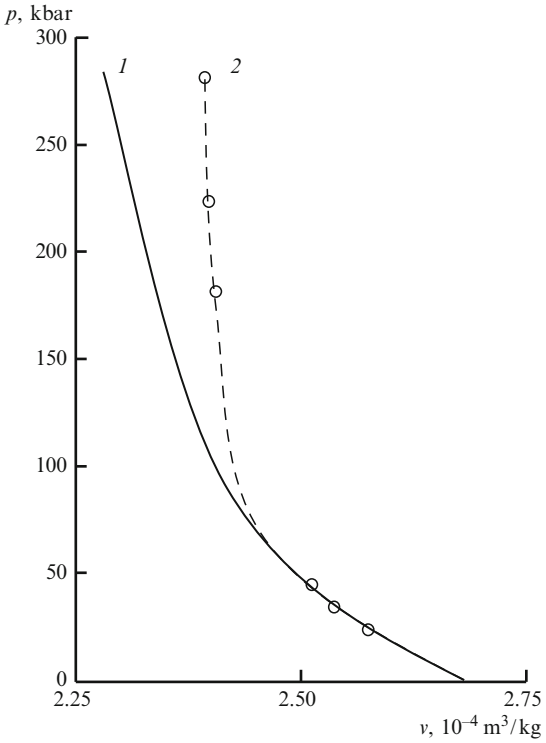

Fig. 5.3. Shock adiabat (*1*) and shock compression curve (*2*) for the Ti–C system (relative density 0.7, grain size 20 μm for Ti and 5 μm for C) [24]

The measured shock velocity in the Mn–S mixture ($2.3 \pm 0.5\,\mathrm{km\,s^{-1}}$) was associated with the action of HE [25]. Preliminary heating of the Zn–Te system up to 150°C was found [26] to increase the velocity of shock from 2.3 to $3.3\,\mathrm{km\,s^{-1}}$ owing to the occurrence of a SSR. Recently, Xu and Thadhani [27] reported on the shock-induced SSR of Ti with Ni accompanied by a volume increase and shock acceleration at 3.2 GPa.

Since 1993, some shock-induced microsecond-scale chemical reactions have been detected with piezoelectric gauges [28–30].

5.2.4 Mechanical Consequences in Recovery Ampoules

The aforementioned experimental techniques are expensive and labor-consuming. For this reason, they are unsuitable for express evaluation of the reaction time in recovery ampoules. Since SSRs take place largely within the axial part of cylindrical ampoules (in the Mach stem, whose diameter depends on the type of energy conversion in a shock), the occurrence/failure of SSRs can be readily inferred from the diameter d and thickness b of the so-called spall plate formed upon explosion [31].

The experiments were carried out as follows. Cylindrical ampoules containing a sample (surrounded by a cylindrical charge of RDX) were placed on a 1-mm-thick steel plate. After explosion, the diameter (d) and the depth (b_{sp}) of the spall on the bottom of the recovery ampoule were measured.

For instance, the shock compression of Sn–S ($D_0 = 6.2\,\mathrm{km\,s^{-1}}$) gave $d = 2.5\,\mathrm{mm}$ and $b_{sp} = 1.5\,\mathrm{mm}$, while that of SnS (an inert compound) gave $d = 1\,\mathrm{mm}$ and $b_{sp} = 0.5\,\mathrm{mm}$ (the velocity of the spall plate being $4.2\,\mathrm{km\,s^{-1}}$ in both experiments). According to our estimates, the kinetic energy of the spall plate (per mole of SnS) attained a value of 60 and $3\,\mathrm{kJ\,mol^{-1}}$, respectively. The difference ($57\,\mathrm{kJ\,mol^{-1}}$, or $0.3\Delta H_r$) is input to the power of the Mach wave. Since the yield of SnS in the Mach stem is also about 0.3 (see Sects. 5.2.2, 5.2.3), the technique described above can be used as a method for express evaluation.

Similar experiments with the Ti–C ($D_0 = 6.2\,\mathrm{km\,s^{-1}}$) and Zn–S ($D_0 = 7.2\,\mathrm{km\,s^{-1}}$) systems [32] have led to formation of TiC and ZnS in yields of 7 and 90%, respectively.

5.2.5 Solid–Solid Syntheses

The formation of high-pressure phases can be regarded as evidence for the occurrence of chemical reactions within the high-pressure zone. The known SSRs can be subdivided into the reactions of decomposition and synthesis. Decomposition reactions require no mass transport and can proceed exceedingly fast. In contrast, synthesis reactions need some time for the dispersion of matter, intermixing, and growth of product grains.

Since water under high pressure is known to acquire the properties of acid, it can be expected to dissolve the metals preceding hydrogen in the electrochemical series. We carried out [33,34] the shock compression of a frozen (with liquid nitrogen) suspension of Zn powder in water in a cylindrical recovery ampoule ($D_0 \geq 6.2\,\mathrm{km\,s^{-1}}$). Analysis of the recovered product showed formation of ZnO in the reaction $\mathrm{Zn + H_2O \rightarrow ZnO + H_2}$.

Similar behavior was exhibited by other acid-soluble metals (B, Al, Ga, Ge, Ti, Zr, Nb, Cr, Mo, W, Mn) [33, 34]. To reduce the residual temperature, the experiments [35] were carried out as shown in Fig. 5.4: products of shock compression were scattered into a big container. In this geometry, we synthesized the cubic (high-pressure) phase of $\mathrm{ZrO_2}$ [35].

In the same year, Sekine [36] synthesized hexagonal diamond (lonsdaleite) through the shock-induced reaction $\mathrm{MgCO_3 + Fe \rightarrow MgO + FeO + C}$.

The data given above demonstrate that shock-induced SSRs can actually occur on a microsecond time scale.

Let us now consider additional evidence for the shock wave character of SSRs. Shock wave experiments can also be used to enter the region of negative pressures (stretching material until it fails). In this region, phase transformations may lead to the formation of loose material and structures that cannot

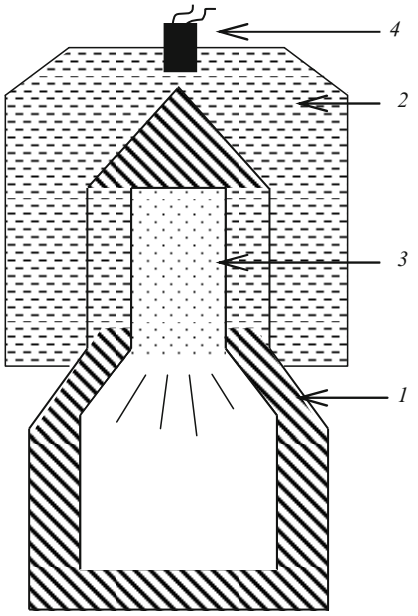

Fig. 5.4. Shock experiments with quenching of products upon scattering. *1* recovery ampoule, *2* high explosive, *3* mixture under study, *4* detonator [33, 34]

form at $p \geq 0$. Back in 1965, we carried out the shock compression of turbostratic BN to obtain a new modification of BN termed the "E phase" (from "explosion") [37]. Later, the synthesis of E-BN was reproduced by other workers [38–44].

$$\text{E-BN}: \ a = 11.14,\ b = 8.06,\ c = 7.40\,\text{Å},\ \rho = 2.50\,\text{g cm}^{-3}$$
$$\text{C}_{60}: \ a = 11.16,\ b = 8.17,\ c = 7.58\,\text{Å},\ \rho = 2.50\,\text{g cm}^{-3}$$

The cell parameters and the density of E-BN are close to those of the fullerene C_{60} synthesized 20 years later [45]. The stabilization of E-BN requires the presence of several percent boron oxide [46].

The shock compression of Nd_2O_3 led to the synthesis of E-Nd_2O_3 [47]. The spectral data show the presence of SiO_2 (approximately 30 wt%) originating from the spalls split from the bottom and walls of the recovery ampoule. The density of E-Nd_2O_3 is as low as $1.6\,\text{g cm}^{-3}$ (cf. $7.42\,\text{g cm}^{-3}$ for Nd_2O_3 and $2.65\,\text{g cm}^{-3}$ for quartz). A very small number of single crystals were also isolated. They had a monoclinic unit cell ($a = 7.5,\ b = 8.7,\ c = 10.3\,\text{Å},\ \beta = 104°$) and very low refractive indices ($n_\text{g} = 1.57,\ n_\text{m} = 1.56,\ n_\text{p} = 1.54$; cf. $n = 2.10$ for Nd_2O_3). This material is insoluble in acids and alkalis and is highly heat resistant (heating is accompanied by reversible thermochromism: from white to violet). The attempts to obtain this compound by shock compression of

Nd_2O_3 mixtures with Si, SiO, or SiO_2 were unsuccessful: at any equivalence ratio, the reaction only yielded neodymium silicates with high ρ and n.

Shock compression of the Zr + 2S mixture in a steel recovery ampoule yielded ZrS_2 with low lattice parameters. Analysis showed that this product is present as the $Zr_{1-x}Fe_xS_2$ solid solution, iron originating from the walls of the recovery ampoule. However, shock compression of the ZrS_2 + Fe mixture did not yield the above-mentioned solid solution [48]. Furthermore, such solid solutions cannot be prepared by heating (upon heating, $Zr_{1-x}Fe_xS_2$ undergoes decomposition into ZrS_2 and FeS).

Shock-induced compression can also be used to synthesize new compounds from reagents with close electronegativity ($\Delta H_r \cong 0$). Kikuchi et al. [49] observed the formation of Ta_2O_5 under shock compression of SiO_2 in a recovery ampoule with tantalum walls, although under normal conditions the redox reaction Ta + SiO_2 is thermodynamically unfavorable.

It is noteworthy that E phases in shock-compressed BN and Nd_2O_3 are only formed in the axial part of a cylindrical recovery ampoule, provided that voids are formed within this area. The latter is a result of tensile stresses arising upon irregular impact of shock waves. Having noticed this fact, we undertook [50, 51] special syntheses of germanium halcogenides in cylindrical ampoules equipped with a large container for scattering shock-compression products (Fig. 5.4). All shock-synthesized compounds (GeSSe, GeSTe, GeSeTe) were found to have ρ values lower than those of thermally synthesized products (and even the original mixtures). Upon heating, these compounds underwent an exothermal transition into normal (higher-density) phases [50,51]. In our laboratory, we succeeded in synthesizing numerous other loosely packed modifications, which opened new horizons for shock chemistry at negative pressures.

Yet another type of "loose" material (foams) can be prepared by shock compression in very strong recovery ampoules. A mixture of the substance under study and a small amount of HE were placed into a cylindrical ampoule. Upon explosion of the outer charge and compression, the inner charge detonated and formed a strong highly porous material. The foam density was found to depend on the substance to HE equivalence ratio [52]. Foams are formed owing to contact melting (gluing) of grains; therefore, this technique is not applicable to the synthesis of high-melting materials (e.g., $MoSi_2$). Nevertheless, for the Mo + 2Si + HE mixture, the ΔH_r value turned out to be sufficient for formation of the $MoSi_2$ foam.

The data given above unequivocally show the feasibility of a SSR within the zone of high pressure or rarefaction on a microsecond time scale. This is also supported by the observation that the exothermic ($\Delta H_r > 0$) reaction within the axial part of the recovery ampoule does not spread over the entire shock-compressed sample. The conversion degree within the Mach stem is about 30%. Had this transformation happened upon unloading, the high temperature attained would have been sufficient for initiation of the reaction over the entire volume of the ampoule. According to [53], this does not happen

owing to the extremely high pressure in the Mach stem, which leads to a decrease in temperature and, accordingly, to a low density of shock-synthesized product.

5.2.6 Mechanism of Ultrafast Diffusion

The aforementioned data require a nontrivial explanation because the velocity of conventional diffusion in solids is several orders of magnitude lower than that which ensures chemical reactions take place on a microsecond time scale. Numerous suggestions have been made regarding possible mechanisms for acceleration of diffusion in shock-compressed materials: large defect concentrations and plastic deformation, heterogeneous heating of components, shear strain, plastic flow to hot spots (as in explosives), and phase transitions in components leading to the breakup of the crystal lattice (hence to a decrease in the activation energy). Although all of these factors do accelerate diffusion, they seem insufficient for explaining the entire set of experimental data.

To rationalize the data, we suggested the fluid-dynamic model of ultrafast (forced) diffusion caused by a difference in the particle velocity of the components in shock-compressed matter [23, 54]. This model has been confirmed experimentally [55–58]. In terms of this model, complete intermixing of particles is achieved owing to penetration of rapidly moving particles into slowly moving particles. The relative velocity of their motion can be determined as follows.

Let us consider rapid compression of some elementary volume of matter from p_0 to some p ($p_0 \ll p$). Given that the compression time $t \ll d/c$ (d is the characteristic diameter of the elementary volume, c is the sound velocity), the work of pressure forces will be roughly equally distributed between the internal and the kinetic energy. The specific kinetic energy will attain an approximate value of

$$\bar{u}^2/2 = -\left(\Delta p/\Delta v\right)/2, \tag{5.1}$$

where $\bar{u}$ is the rms particle velocity.

Expression (5.1) coincides with that determining the particle velocity of a shock [1]; hence, the value of $\bar{u}$ for each reagent of a powder mixture can be estimated from its shock-compression curve. Given that both reagents have identical shock compression curves, their $\bar{u}$ values are identical, so the forced diffusion is nearly absent. Conversely, in the case of different shock adiabats, the forced diffusion does take place. In this case, $\Delta\bar{u}$ can be regarded as the velocity of forced diffusion.

Accordingly, the time of diffusion τ (intermixing), and hence the reaction time, can be estimated from the expression [59]

$$\tau = 2d/\Delta\bar{u}. \tag{5.2}$$

At $\Delta\bar{u} \approx 1\,\mathrm{km\,s^{-1}}$ and $d \approx 0.1\,\mathrm{mm}$, we obtain $\tau \approx 10^{-7}\,\mathrm{s}$. Given that the shock adiabats for Sn, S, and Te are known, we obtain that for the Sn–S mixture

($d = 100\,\mu\text{m}$) a value of $\tau = 0.3\,\mu\text{s}$ can be attained at $p = 10\,\text{GPa}$, while for the Sn–Te mixture ($d = 100\,\mu\text{m}$), a value of $\tau = 0.8\,\mu\text{s}$ can be attained at $p = 50\,\text{GPa}$. These estimates agree reasonably with experiment.

It follows that, under conditions of shock compression, the velocity of forced diffusion can be sufficiently large. This means that the SSD in charges with reasonable dimensions can be expected to occur, provided the thermodynamic criterion suggested in [4] is satisfied.

5.3 Shock-Induced Solid–Solid Detonation in Zinc–Sulfur Powders

As can be inferred from Sect. 5.1, SSD at some certain conditions can be expected to occur when the criterion of detonation ability [4] is satisfied, although the SSD in a given system may proceed exceedingly slowly. But this means that in the systems that do not fit the thermodynamic criterion [4], SSD will never occur in principle.

The criterion [4] can be written in the form

$$Q_{\text{p,v}} > 0 \,\text{or}\, \Delta v_{\text{p,h}} > 0. \tag{5.3}$$

Unfortunately, the reference data necessary for calculating (5.3) are often lacking in the literature. For the Mn–S and Al–S systems, we could perform only rough estimations: the Mn–S system was found to be unsuitable, but the Al–S system was suitable for observation of SSD. We managed to strictly apply criterion (5.3) only to the systems Zn–Se, Zn–Te, Cu–S, Ti–C–Al–paraffin, and Zn–S.

For control experiments, we chose the reaction $\text{Zn} + \text{S} \rightarrow \text{ZnS}$ [60]. We have calculated the parameters of ideal detonation in the compact Zn–S system ($\rho_0 = 3.87\,\text{g cm}^{-3}$): $D_0 = 2{,}500\,\text{m s}^{-1}$, $p_{\text{CJ}} = 3\,\text{GPa}$ [61]. These values are close to those typical of detonation in condensed HEs. The possibility of SSD in the Zn–S system was also supported by the experimental data [62].

We assume that the most convincing evidence for the occurrence of SSD is the reacceleration and intensification of the shock wave in a given medium [4].

5.3.1 Initiation of Detonation

Our preliminary results [61] confirmed the possibility of SSD in Zn–S charges ($\rho_0 = 1.33\,\text{g cm}^{-3}$, $20 \times 20 \times 60\,\text{mm}^3$ in size) placed into a thick-walled (5-mm) steel ampoule tightly closed with a 2-mm cover plate. Explosion was initiated with an electrically exploding wire from the bottom. In this geometry, we observed the following two phenomena.

One was a loud clap and the other was strong plastic deformation of the cover plate (Fig. 5.5). Our rich experience in the field suggests that such a

Fig. 5.5. A deformed cover

deformation can be caused by a pressure of several hundred atmospheres. The resultant temperature of the ampoule was below 50°C.

In other runs, the process proceeded smoothly, without noticeable deformation of the cover plate. The resultant temperature was above 100℃, but below 800℃. The extent of conversion into ZnS attained a value above 80%. According to [61], the former process can be regarded as detonation and the latter one as slow combustion of the Zn–S powder mixture.

In further experiments, we measured wave velocities for both processes. A low velocity can be due to the fact that the detonation develops in two stages: first, only a small amount of the Zn–S mixture reacts, and this wave of incomplete combustion turns off our gauges; then the detonation wave begins to propagate over a preheated mixture.

We have evaluated the lower limit for the pressure p that caused the deformation of the cover (Fig. 5.5): $p = 360$ atm. In the case of a slow reaction, the p value evaluated did not exceed 80 atm.

At present, similar experiments with longer ampoules (where the probability of detonation onset is higher) are in progress.

5.3.2 Direct Measurement of Detonation Velocity

In our experiments [63], we used an equimolar powder mixture of Zn and S. The highly exothermic reaction $\mathrm{Zn} + \mathrm{S} \rightarrow \mathrm{ZnS}$ proceeds without gas evolution and, *owing to thermal expansion of the product*, satisfies condition (5.3). The particle size of Zn and S powders was 3–5 μm, while the sample density (ρ) was 0.6–0.7 of the theoretical value.

The experimental setup is shown in Fig. 5.6. A mixture was pelleted into cylinders 16.5 mm in diameter and 40–200 mm long. Samples were placed in a tubular container made of a porous composite (with a low velocity of sound) to exclude the effect of elastic waves in the container walls on the results

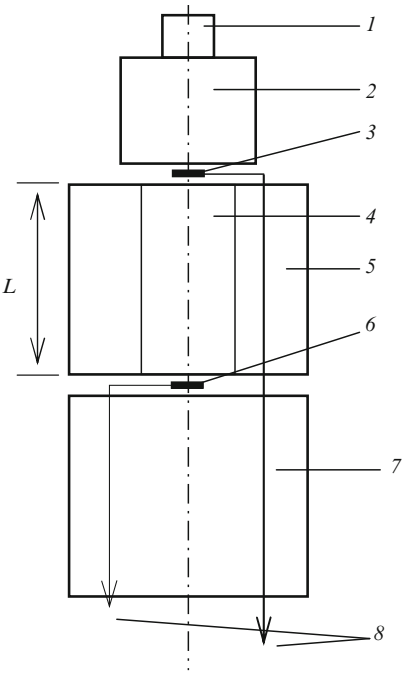

Fig. 5.6. Experimental setup. *1* detonator, *2* high explosive, *3*, *6* contact sensors, *4* Zn–S sample, *5* container (made of porous composite), *7* stand, *8* wire leads to oscilloscopes, L gauge length

of the measurements. Shocks were generated by detonation of the charge (TNT/RDX, 40 mm in diameter, 35 mm in height, $D_0 = 7.85\,\mathrm{km\,s^{-1}}$). In experiments, we measured the time interval τ between the arrival of the shock at sensors (contact gauges). To avoid the sample discontinuity, the gauges were only placed on the sample top and bottom. The average velocity of shock propagation through a sample was determined from the expression $\bar{D} = L/\tau$. For a sensor thickness of 200 μm, the contact gap was 100 μm. The estimated measurement error (δ) was 0.6% at $L = 40$ mm and 0.1% at $L = 200$ mm. Signals from the sensors were recorded with two oscilloscopes (Tektronix TDS 1012). The experiments were carried out at 14℃. The data obtained are presented in Table 5.1.

In the absence of a chemical reaction, the shock wave generated in the sample could be expected to decay at a distance of 25–30 mm from the top. So, a minimal sample length (40 mm) was chosen so that in the absence of chemical replenishment the sensor numbered 6 in Fig. 5.6 would give no signal at all. Experimental data for the trials when both sensors produced signals are presented in Table 5.1. These data suggest that the process of shock propagation was supported by the energy released in the chemical reaction taking place in the zone of high dynamic pressure.

Table 5.1. Experimental data for direct measurement of detonation velocity

Experimental run	L (mm)	$\bar{D}$ ($\mathrm{km\,s^{-1}}$)	ρ (%)	δ (%)
1	40	2.27	68.1	0.6
2	60	1.30	63.0	0.2
3	75	1.64	71.6	0.2
4	90	1.39	60.7	0.2
5	100	2.55	62.4	0.2
6	150	2.195	63.5	0.1
7	150	1.915	62.4	0.1
8	200	2.169	59.4	0.1

As follows from Table 5.1, the shock velocity $\bar{D}$ initially drops sharply from a starting value of $7.85\,\mathrm{km\,s^{-1}}$ at the bottom of the charge to $1.30\,\mathrm{km\,s^{-1}}$ (at $L = 60\,\mathrm{mm}$) and then increases to above $2\,\mathrm{km\,s^{-1}}$ (for $L = 100$–$200\,\mathrm{mm}$). Some scattering can be attributed (a) to a random character of detonation initiation at some points behind the shock wave front, (b) possible occurrence of several detonation modes and transition processes between them [64], and (c) some variation in the induction period for the chemical reaction. Theoretical estimation for an ideal detonation in the monolith matter under study gives a value of $D_0 = 2.486\,\mathrm{km\,s^{-1}}$ [61]. If we take into consideration that in our experiments $\rho = 60$–70%, the measured $\bar{D}$ values agree well with the theoretical prediction for the detonation process.

The X-ray diffraction data for the products taken at the bottom of the container (numbered 5 in Fig. 5.6) are indicative of virtually complete conversion of the starting mixture into ZnS (only trace amounts of Zn were detected), which confirms the occurrence of a chemical reaction within the shock. The effects of high temperature were also noticed on the surface of the sensor numbered 6 in Fig. 5.6, which also supports the occurrence of a highly exothermic reaction.

The observed acceleration of the shock can be regarded as experimental evidence for the occurrence of SSD in the system under consideration. When we record a steady propagation of shock, there always exists a probability that the observed process is weakly decaying and hence is not self-sustaining, but the experimental accuracy is not sufficient to observe this on a limited gauge length. In contrast, the observation of acceleration (as in our experiments) leaves no grounds for doubting the occurrence of detonation in the material under study.

SSD can be regarded as a new type of transport phenomenon in reactive media. The phenomenon may find an application (e.g., in mining) where the shattering action of explosives is being used while the presence of gaseous products is not desirable. Just like solid-state synthesis by combustion, detonation-mediated synthesis in the solid state may also prove useful for preparation of various compounds and materials.

5.4 Thermodynamic Fundamentals of Solid–Solid Detonation

5.4.1 Basic Assumptions

The general theory of shock wave processes [2] does not differentiate between gases and condensed media, including powder systems. In numerous monographs on condensed HEs (e.g., [64, 65]), little or no attention has been given to the thermochemical aspects of shock wave processes. In this section, we will try to fill this gap.

The notion of the thermal effect of a reaction is basic in the physics of explosions [64, 65]. Meanwhile, this notion has not been strictly defined yet in relation to shock wave processes. To fill this gap, let us apply the first law of thermodynamics to an element or microscopic particle of a reactive medium. For irreversible processes starting in the metastable state, it can be written in the form

$$\Delta e = \Delta q - \Delta A. \tag{5.4}$$

Expression (5.4) follows from the classical definition of internal energy [2, 66]: the specific internal energy e is a specific measure of the entire internal motion in the element under consideration, including the energy of chemical bonds.

Let us consider the consequences of (5.4) under the following assumptions adopted in thermochemistry:

(a) The mechanical work A in (5.4) is defined by the expression

$$\mathrm{d}A = -p\,\mathrm{d}v. \tag{5.5}$$

(b) In our case, local thermodynamic states of matter can be assumed to be in equilibrium or quasi-equilibrium (metastable). For each of these states, the following thermodynamic functions (variables) can be defined: specific internal energy e, pressure p, specific volume v or density $\rho = 1/v$, absolute temperature T, and specific entropy s. Accordingly, the following relationships hold: $p \geq 0,\ v > 0,\ s \geq 0,\ T \geq 0$ and $s = 0$ at $T = 0$.

(c) Each local thermodynamic state is completely defined by a finite number of parameters. First, these are any pair of the above thermodynamic variables which fully define only equilibrium states of medium. Second, this is some set ($n \geq 1$) of independent scalar inner characteristics of matter (chemical/phase composition, porosity, grain size, etc.). The chemical/phase composition can be characterized by a set of parameters written in the form $\langle\eta\rangle = \langle\eta_1,\ \eta_2,\ \eta_3, \ldots,\ \eta_n\rangle$.
For nonequilibrium states, all the functions of a local thermodynamic state, by definition, are the function of the $n + 2$ parameters above. For instance,

$$e = e(s, v, \langle\eta\rangle) = e(p, v, \langle\eta\rangle) = e(p, T, \langle\eta\rangle) = e(v, T, \langle\eta\rangle), \tag{5.6}$$

where the variables s, v, p, and T refer to the same state of matter.

(d) The choice of the n independent characteristics above is ambiguous. Among all possible sets $\langle\eta\rangle$, there exists at least one for which, at $\langle\eta\rangle = \text{const}$, the thermodynamic parameters satisfy the same expressions that are valid for equilibrium states. Let us term such a set the "inner variables." Hereinafter, such a set $\langle\eta\rangle$ will be regarded as a unique characteristic of a physicochemical transformation in the system under consideration.
Therefore, the following relationships will be assumed to hold:

$$T = \left(\frac{\partial e}{\partial s}\right)_{v,\langle\eta\rangle}, \; p = -\left(\frac{\partial e}{\partial v}\right)_{s,\langle\eta\rangle}, \tag{5.7}$$

$$c_p = T\left(\frac{\partial s}{\partial T}\right)_{p,\langle\eta\rangle} \geq c_v = T\left(\frac{\partial s}{\partial T}\right)_{v,\langle\eta\rangle} \geq 0, \tag{5.8}$$

$$\left(\frac{\partial p}{\partial v}\right)_{s,\langle\eta\rangle} \leqslant \left(\frac{\partial p}{\partial v}\right)_{T,\langle\eta\rangle} \leqslant 0. \tag{5.9}$$

For equilibrium $\langle\eta\rangle$, there is no need for a partial derivative at $\langle\eta\rangle$.

(e) We will consider only conventional media that obey relations (5.10)–(5.12):

$$\beta = \frac{1}{v}\left(\frac{\partial v}{\partial T}\right)_{p,\langle\eta\rangle} > 0\,, \quad \left(\frac{\partial p}{\partial T}\right)_{v,\langle\eta\rangle} > 0\,, \quad \left(\frac{\partial e}{\partial p}\right)_{v,\langle\eta\rangle} > 0\,, \tag{5.10}$$

where β is the volumetric coefficient of thermal expansion,

$$\left(\frac{\partial e}{\partial v}\right)_{p,\langle\eta\rangle} > 0\,, \tag{5.11}$$

$$\left(\frac{\partial^2 p}{\partial v^2}\right)_{s,\langle\eta\rangle} > 0. \tag{5.12}$$

To date, assumptions a–d seem reasonable only in cases of homogeneous media for which the concentration of components can be regarded as an internal thermodynamic variable. Meanwhile, the physical meaning of internal variables is of no significance for our analysis. This implies that the results obtained are applicable to any system satisfying assumptions a–e.

5.4.2 Thermal Effects of Physicochemical Transformation

For a given transformation $\langle\eta_0\rangle \to \langle\eta\rangle$, we can obtain different thermal characteristics of the process from (5.4) and (5.5).

Physicochemical transformations are normally characterized by the thermal effects $Q_v \equiv Q_{v,T}$ (at v, $T = \text{const}$) or $\Delta H_\text{r} \equiv Q_p \equiv Q_{p,T}$ (at p, $T = \text{const}$). According to (5.4) and (5.5), these terms can be defined as

$$Q_{v,T} = e_0 - e(v_0, T_0, \langle\eta\rangle), \tag{5.13}$$

$$Q_{p,T} = e_0 - e(p_0, T_0, \langle\eta\rangle) - p_0 \Delta v_{p,T}, \tag{5.14}$$

where $e_0 = e(V_0, T_0, \langle\eta_0\rangle) = e(p_0, T_0, \langle\eta_0\rangle) = e(p_0, v_0, \langle\eta_0\rangle$ and $\Delta v_{p,T}$ is the increment in the specific volume during the transformation $\langle\eta_0\rangle \to \langle\eta\rangle$ at given p_0 and T_0. Transformations (media) satisfying the conditions $Q_{v,T} > 0$, $Q_{p,T} > 0$ are termed "exothermic."

It was suggested [67] characterizing chemical reactions in shock wave processes by the value of $Q_{p,v}$:

$$Q_{p,v} = e_0 - e\,(p_0, v_0, \langle\eta\rangle)\,. \tag{5.15}$$

According to [67], the sign of $Q_{p,v}$ defines the type of shock (see later).

Still another heat parameter of the chemical transformation $\langle\eta_0\rangle \to \langle\eta\rangle$, the value of Q_{cal} (calorimetric), can be defined as

$$Q_{\text{cal}} = e_0 - e\,(p_0, T_0, \langle\eta\rangle)\,. \tag{5.16}$$

It is the value of Q_{cal} that is measured in experiments with calorimetric bombs. From (5.14) and (5.16), we obtain

$$Q_{\text{cal}} - Q_{p,T} = p_0 \Delta v_{p,T}. \tag{5.17}$$

This expression is used to determine $Q_{p,T}$ from a measured value of Q_{cal}.

The thermal effects $Q_{v,T}$, $Q_{p,T}$, $Q_{p,v}$, and Q_{cal} may turn out to be identical in their magnitude. According to (5.13)–(5.16), this may happen only as a rare case when $\Delta v_{p,T} = 0$. But when $\Delta v_{p,T} \neq 0$, these thermal effects have different magnitudes. This can be demonstrated by using the diagram presented in Fig. 5.7.

A situation here corresponds to the inequality $\Delta v_{p,T} > 0$ (e.g., numerous exothermic SSRs, decomposition of HE, or combustion of some gaseous mixtures). The $\langle\eta_0\rangle \to \langle\eta\rangle$ processes taking place at v, $T = \text{const}$ or p, $T = \text{const}$ correspond to the solid arrows between the point (p_0, v_0) and the end points (p_1, v_0) and (p_0, v_2), respectively. According to (5.13) and (5.14), the end points belong to the isotherm line T_0 of the product. For $\Delta v_{p,T} > 0$, we have $v_2 > v_0$. In virtue of inequality (5.9), $(\partial p/\partial v)_{T,\langle\eta\rangle} \leqslant 0$, it follows that $p_1 > p_0$. The $\langle\eta_0\rangle \to \langle\eta\rangle$ process taking place at p, $v = \text{const}$ is presented by the point (p_0, v_0).

The $\langle\eta_0\rangle \to \langle\eta\rangle$ process in a calorimetric bomb corresponds to the dashed arrow between the point (p_0,v_0) and the end point (p_3,v_3) on the isotherm line T_0. In such experiments, the magnitude of q is normally determined as $q = e_0 - e_3$. It is well known that the weight and volume of a sample are taken to be much smaller than the weight and inner volume of a bomb. Hence, in the case of a SSR, $p_3 = p_0$, $v_3 = v_2$, and $e_3 = e(p_0, v_2, \langle\eta\rangle) \equiv e(p_0, T_0, \langle\eta\rangle)$. In the case of HE decomposition, the product can be regarded as an ideal gas between points 2 and 3 in Fig. 5.7. Then according to the thermodynamic identity

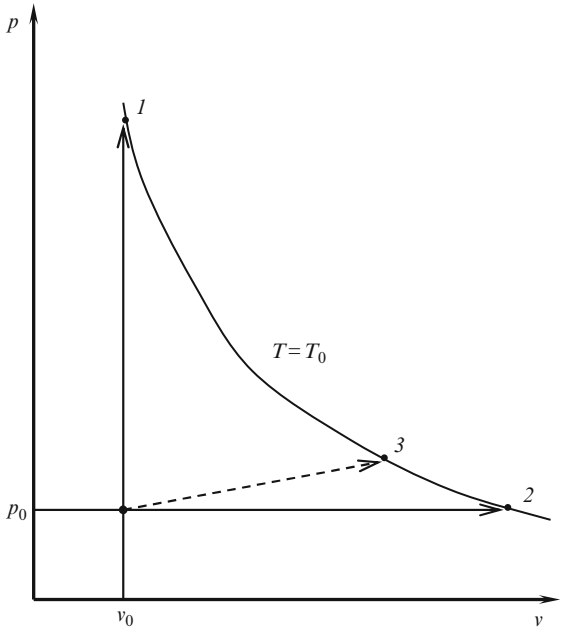

Fig. 5.7. States during transformation of matter for $\Delta v_{p,T} > 0$. *1* point $(p_1,\ v_0)$, *2* point $(p_0,\ v_2)$, *3* point $(p_3,\ v_3)$

$$\left(\frac{\partial e}{\partial v}\right)_{T,\langle\eta\rangle} = T\left(\frac{\partial p}{\partial T}\right)_{v,\langle\eta\rangle} - p \tag{5.18}$$

and the Clapeyron equation, $(\partial e/\partial v)_{T,}\langle\eta\rangle = 0$. Therefore, $e_3 = e(p_3, v_3,\ \langle\eta\rangle) = e(p_0, v_2,\ \langle\eta\rangle) \equiv e(p_0, T_0,\ \langle\eta\rangle)$. According to (5.16), in both cases we obtain $Q_{\text{cal}} = e_0 - e_3 = q$. In other words, experiments with calorimetric bombs indeed yield the values of Q_{cal}.

In publications on the physics of explosions, one often comes across the expression (5.17) in which $Q_v \equiv Q_{v,T}$ is used instead of Q_{cal}, without any indication of the specificity of the equation of state for products and the initial state $(p_0,\ v_0,\ \langle\eta_0\rangle)$. Actually, it is assumed the equalities $Q_{\text{cal}} = Q_{v,T}$ and $e_3 = e_1$ [see (5.13), (5.16)] always hold true. In reality, this is possible only when $(\partial e/\partial v)_{T,}\langle\eta\rangle = 0$ over the entire segment of the isotherm T_0 between points 1 and 2 in Fig. 5.7. In the case of dense gases and condensed media, this condition is certainly not fulfilled. This can be demonstrated by transforming the right-hand side of (5.18) by using the van der Waals equation for dense gases or the inequality $(\partial^2 p/\partial T^2)_{v,\langle\eta\rangle} > 0$, valid for most condensed media at low temperatures [66]. Therefore, for shock wave processes in condensed media, $Q_{\text{cal}} \neq Q_{v,T}$.

In Fig. 5.7, the state of the reaction product $(p_0,\ v_0,\ \langle\eta\rangle)$ satisfies the inequalities $p_0 < p_1$ and $v_0 < v_2$; therefore, it follows from (5.10) and (5.11)

that $e(p_0, v_0, \langle\eta\rangle) < e_1$ and $e(p_0, v_0, \langle\eta\rangle) < e_2$. Accordingly, from (5.13), (5.15), and (5.16), we obtain $Q_{p,v} > Q_{v,T}$ and $Q_{p,v} > Q_{\text{cal}}$.

Having plotted a similar diagram for $\Delta v_{p,T} < 0$, one can be convinced that in this case the thermal effects $Q_{v,T}$, $Q_{p,T}$, $Q_{p,v}$, and Q_{cal} (5.13)–(5.16) also have different values.

The values of $Q_{v,T}$, $Q_{p,T}$, and $Q_{p,v}$ normally have the same sign, although there are some exclusions. An example is combustion of the thermite system $3Fe_3O_4 + 8Al$. At $p = 1\,\text{atm}$, the combustion temperature rises. To ensure $T = \text{const}$, one has to expel some heat. Then according to (5.4), (5.5), and (5.14), $Q_{p,T} > 0$. But this is accompanied by a volume decrease which has to be replenished upon additional supply of heat. Hence, from (5.4), (5.5), and (5.15), it follows that $Q_{p,v} < 0$ [67].

Therefore, the transformation $\langle\eta_0\rangle \to \langle\eta\rangle$ can be characterized by at least four thermal effects (5.13)–(5.16) having different physical meaning and magnitude. Let us analyze their role in shock wave processes taking place in reactive media. We will begin with a relation between the mechanical and thermodynamic parameters of shocked matter.

5.4.3 Shock Equations

In the reference system attached to the shock, let us consider an elementary cylindrical volume of matter as shown in Fig. 5.8. Applying the conservation of mass and momentum to this element [2], we come to the well-known relationships for the shock:

$$\rho_0 D = \rho\,(D - u)\,, \tag{5.19}$$

$$p - p_0 = \rho_0 D u. \tag{5.20}$$

Applying the principle of energy conservation (upon neglect of heat exchange between elementary volumes, as adopted for very fast processes), we obtain

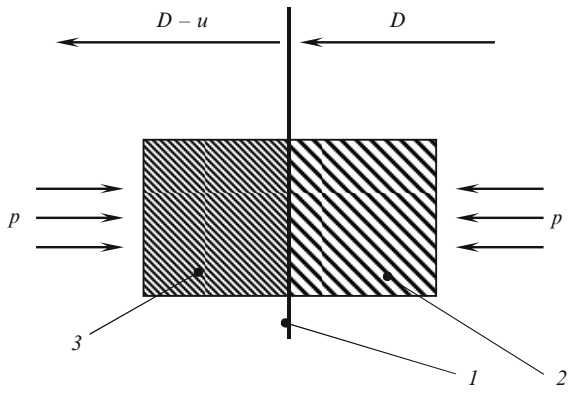

Fig. 5.8. Deriving the shock equation. *1* shock wave, *2* undisturbed material, *3* compressed material

$$\rho_0 D\,(\Delta e + \Delta K) = p_0 D - p\,(D - u)\,,$$

where K is the specific kinetic energy. Introducing $\Delta e = e - e_0$, $\Delta K = (D-u)^2/2 - D^2/2$, and excluding D and u [through the use of (5.19), (5.20)], we obtain

$$e\,(p, v, \langle\eta\rangle) - e_0 = (p - p_0)\,(v_0 - v)\,/2. \tag{5.21}$$

For the classical definition of e [2, 66], this expression is applicable to shocks with or without transformations [2].

At constant $\langle\eta\rangle$, expression (5.21) describes a family of curves (termed "dynamic adiabats") in the coordinates p–v. According to (5.9)–(5.12), the dynamic adiabats have the form shown in Fig. 5.9 [2].

The character of shock motion in reactive media is known [2] to depend on the position of the adiabat relative to the point (p_0, v_0). This position can be predicted by applying simple criteria (5.3). These criteria can be derived as follows. In view of (5.15), expression (5.21) can be written in the form

$$e(p, v, \langle\eta\rangle) - e(p_0, v_0, \langle\eta\rangle) = (p - p_0)\,(v_0 - v)\,/2 + Q_{p,v}. \tag{5.22}$$

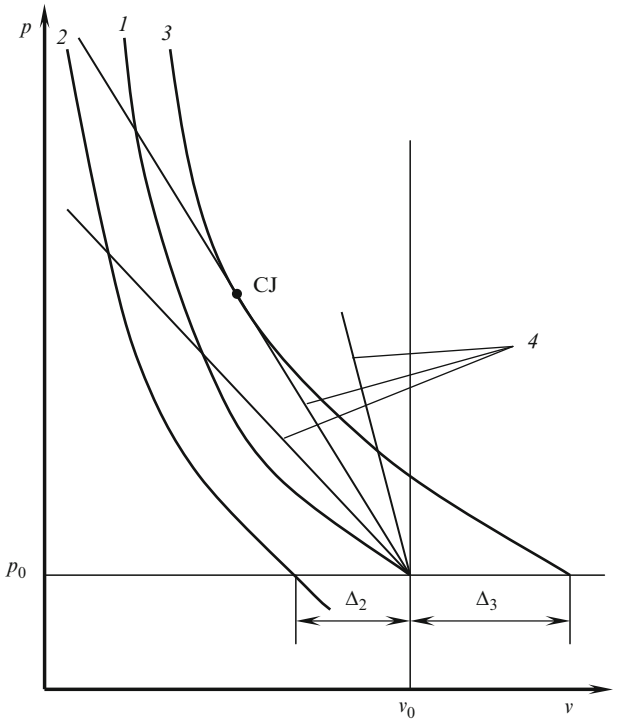

Fig. 5.9. The dynamic adiabats. *1* shock adiabat ($Q_{p,v} = 0$, $\Delta v_{p,h} = 0$), *2* shock adiabat ($Q_{p,v} < 0$, $\Delta v_{p,h} = -\Delta_2 < 0$), *3* detonation adiabat ($Q_{p,v} > 0$, $\Delta v_{p,h} = \Delta_3 > 0$), *4* Rayleigh lines

In (5.22), $Q_{p,v}$ is constant (since it depends on p_0, v_0, $\langle\eta_0\rangle$, and $\langle\eta\rangle$, which are assumed to be constant). This parameter defines a position of the dynamic adiabat relative to the point (p_0, v_0). For $Q_{p,v} < 0$, the adiabat intersects the isobar line p_0 for $v < v_0$ (Fig. 5.9); at $Q_{p,v} = 0$, it passes through the point (p_0, v_0); while for $Q_{p,v} > 0$, it crosses the isobar line p_0 for $v > v_0$ and the isochore line v_0 for $p > p_0$.

Introducing $Q_{v,T}$ (5.13), $Q_{p,T}$ (5.14), or Q_{cal} (5.16) into (5.21), we arrive at a complicated expression that is inconvenient for deriving a simple criterion for the position of the dynamic adiabat relative to the point (p_0, v_0). This implies that *it is the thermal effect* $Q_{p,v}$ (5.15) *that defines the motion of a shock wave in reactive systems.*

Now let us derive another criterion for position of the dynamic adiabat relative to (p_0, v_0). Introducing $p = p_0$ into (5.21) and performing some transformations, we obtain

$$h\left(p_0, v, \langle\eta\rangle\right) = h\left(p_0, v_0, \langle\eta_0\rangle\right), \tag{5.23}$$

where $h(p, v,\ \langle\eta\rangle) = e(p, v,\ \langle\eta\rangle) + pv$ is the specific enthalpy for the matter under consideration. Equation (5.23) defines the point v at which the dynamic adiabat (5.21) intersects the isobar line p_0 (Fig. 5.9). We may also introduce the volume effect of physicochemical transformation:

$$\Delta v_{p,h} = v - v_0 \text{ at } p = \text{const}, \; h = \text{const}. \tag{5.24}$$

This is the increment in the specific volume of a medium in the real or imaginary process $\langle\eta_0\rangle \to \langle\eta\rangle$ taking place at $p_0 = \text{const}$ under adiabatic conditions. In any case, $\Delta v_{p,h}$ is not identical to $\Delta v_{p,T}$. These magnitudes may even have different signs. For example, for a stoichiometric mixture of H_2 with O_2, $\Delta v_{p,h} > 0$, while $\Delta v_{p,T} < 0$.

The value of $\Delta v_{p,h}$ defines the position of the dynamic adiabat relative to the point (p_0, v_0). For $\Delta v_{p,h} < 0$ (Fig. 5.9), the dynamic adiabat intersects the isobar line p_0 for $v < v_0$; at $\Delta v_{p,h} = 0$, it passes through the point (p_0, v_0); and for $\Delta v_{p,h} > 0$, it intersects the isobar line p_0 for $v > v_0$ and the isochore line v_0 for $p > p_0$ (Fig. 5.9). Therefore, the signs of $Q_{p,v}$ and $\Delta v_{p,h}$ are identical. For this reason, both criteria in (5.3) are equivalent.

5.4.4 The Role of Thermal Effects in Laminar Motion of Reacting Matter

Now let us consider the role of the aforementioned four thermal effects in the motion of reactive particles behind the shock. According to (5.4) and (5.5), for an element of a medium, we can write

$$\frac{\mathrm{d}e}{\mathrm{d}t} = \frac{\mathrm{d}q}{\mathrm{d}t} - p\frac{\mathrm{d}v}{\mathrm{d}t}. \tag{5.25}$$

On the other hand, since e is a function of p, v, and $\langle\eta\rangle$, we obtain

$$\frac{\mathrm{d}e}{\mathrm{d}t} = \left(\frac{\partial e}{\partial p}\right)_{v,\langle\eta\rangle} \frac{\mathrm{d}p}{\mathrm{d}t} + \left(\frac{\partial e}{\partial v}\right)_{p,\langle\eta\rangle} \frac{\mathrm{d}v}{\mathrm{d}t} + \left(\frac{\partial e}{\partial\langle\eta\rangle}\right)_{p,v} \frac{\mathrm{d}\langle\eta\rangle}{\mathrm{d}t}. \tag{5.26}$$

Here and hereinafter we will admit that

$$\left(\frac{\partial Z}{\partial\langle\eta\rangle}\right)_{X,Y} \frac{\mathrm{d}\langle\eta\rangle}{\mathrm{d}t} = \sum_{i=1}^{n} \left(\frac{\partial Z}{\partial\eta_i}\right)_{X,Y} \frac{\mathrm{d}\eta_i}{\mathrm{d}t},$$

where Z stands for e or v while X and Y stand for p, v, or T.

The last term in (5.26) (taken with the opposite sign) can be regarded as the rate of heat evolution at p, $v = \mathrm{const}$ [cf. (5.15)]:

$$\frac{\mathrm{d}Q_{p,v}}{\mathrm{d}t} = -\left(\frac{\partial e}{\partial <\eta>}\right)_{p,v} \frac{\mathrm{d}<\eta>}{\mathrm{d}t}.$$

Using the thermodynamic identity

$$\left(\frac{\partial p}{\partial v}\right)_{s,\langle\eta\rangle} = -\left(\left(\frac{\partial e}{\partial v}\right)_{p,\langle\eta\rangle} + p\right)\left(\frac{\partial p}{\partial e}\right)_{v,\langle\eta\rangle},$$

and the expression for the Grüneisen coefficient

$$\Gamma = v\left(\frac{\partial p}{\partial e}\right)_{v,\langle\eta\rangle},$$

we obtain

$$\frac{\mathrm{d}p}{\mathrm{d}t} = \left(\frac{\partial p}{\partial v}\right)_{s,\langle\eta\rangle} \frac{\mathrm{d}v}{\mathrm{d}t} + \frac{\Gamma}{v}\left(\frac{\mathrm{d}Q_{p,v}}{\mathrm{d}t} + \frac{\mathrm{d}q}{\mathrm{d}t}\right). \tag{5.27}$$

Therefore, the relation between $\mathrm{d}p$ and $\mathrm{d}v$ is defined by the derivative of $(Q_{p,v} + q)$. In other words, the thermal effect $Q_{p,v}$ (5.15) plays a part similar to that of externally supplied heat q.

For e as a function of v, T, and $\langle\eta\rangle$, we obtain

$$\frac{\mathrm{d}e}{\mathrm{d}t} = \left(\frac{\partial e}{\partial v}\right)_{T,\langle\eta\rangle} \frac{\mathrm{d}v}{\mathrm{d}t} + \left(\frac{\partial e}{\partial T}\right)_{v,\langle\eta\rangle} \frac{\mathrm{d}T}{\mathrm{d}t} + \left(\frac{\partial e}{\partial\langle\eta\rangle}\right)_{v,T} \frac{\mathrm{d}\langle\eta\rangle}{\mathrm{d}t}. \tag{5.28}$$

Combining (5.25) with (5.28), taking into account that $c_v = (\partial e/\partial T)_{v,\langle\nu\rangle}$and [cf. (5.13)]

$$\frac{\mathrm{d}Q_{v,T}}{\mathrm{d}t} = -\left(\frac{\partial e}{\partial\langle\eta\rangle}\right)_{v,T} \frac{\mathrm{d}\langle\eta\rangle}{\mathrm{d}t},$$

from the thermodynamic identity

$$\left(\frac{\partial T}{\partial v}\right)_{s,\langle\eta\rangle} = -\left(\left(\frac{\partial e}{\partial v}\right)_{T,\langle\eta\rangle} + p\right)\frac{1}{c_v},$$

we obtain

$$\frac{\mathrm{d}T}{\mathrm{d}t} = \left(\frac{\partial T}{\partial v}\right)_{s,\langle\eta\rangle} \frac{\mathrm{d}v}{\mathrm{d}t} + \frac{1}{c_v}\left(\frac{\mathrm{d}Q_{v,T}}{\mathrm{d}t} + \frac{\mathrm{d}q}{\mathrm{d}t}\right). \tag{5.29}$$

Therefore, the relation between $\mathrm{d}T$ and $\mathrm{d}v$ is equally defined by the values of q and $Q_{v,T}$ (5.13).

Since v and e are functions of p, T, and $\langle\eta\rangle$, we obtain

$$\frac{\mathrm{d}v}{\mathrm{d}t} = \left(\frac{\partial v}{\partial p}\right)_{T,\langle\eta\rangle} \frac{\mathrm{d}p}{\mathrm{d}t} + \left(\frac{\partial v}{\partial T}\right)_{p,\langle\eta\rangle} \frac{\mathrm{d}T}{\mathrm{d}t} + \left(\frac{\partial v}{\partial\langle\eta\rangle}\right)_{p,T} \frac{\mathrm{d}\langle\eta\rangle}{\mathrm{d}t}, \tag{5.30}$$

$$\frac{\mathrm{d}e}{\mathrm{d}t} = \left(\frac{\partial e}{\partial p}\right)_{T,\langle\eta\rangle} \frac{\mathrm{d}p}{\mathrm{d}t} + \left(\frac{\partial e}{\partial T}\right)_{p,\langle\eta\rangle} \frac{\mathrm{d}T}{\mathrm{d}t} + \left(\frac{\partial e}{\partial\langle\eta\rangle}\right)_{p,T} \frac{\mathrm{d}\langle\eta\rangle}{\mathrm{d}t}. \tag{5.31}$$

Combining (5.25), (5.30), (5.31), and

$$\frac{\mathrm{d}Q_{p,T}}{\mathrm{d}t} = -\left(\frac{\partial e}{\partial\langle\eta\rangle}\right)_{p,v} \frac{\mathrm{d}\langle\eta\rangle}{\mathrm{d}t} - p\left(\frac{\partial v}{\partial\langle\eta\rangle}\right)_{p,v} \frac{\mathrm{d}\langle\eta\rangle}{\mathrm{d}t}$$

[cf. (5.14)], from

$$c_p = \left(\frac{\partial e}{\partial T}\right)_{p,\langle\nu\rangle} + p\left(\frac{\partial v}{\partial T}\right)_{p,\langle\nu\rangle}$$

and the thermodynamic identity

$$\left(\frac{\partial T}{\partial p}\right)_{s,\langle\eta\rangle} = -\left(\left(\frac{\partial e}{\partial p}\right)_{T,\langle\eta\rangle} + p\left(\frac{\partial v}{\partial p}\right)_{T,\langle\eta\rangle}\right)\frac{1}{c_p},$$

we obtain

$$\frac{\mathrm{d}T}{\mathrm{d}t} = \left(\frac{\partial T}{\partial p}\right)_{s,\langle\eta\rangle} \frac{\mathrm{d}p}{\mathrm{d}t} + \frac{1}{c_p}\left(\frac{\mathrm{d}Q_{p,T}}{\mathrm{d}t} + \frac{\mathrm{d}q}{\mathrm{d}t}\right). \tag{5.32}$$

Here a similar role is played by q and $Q_{p,T}$.

Note that in deriving (5.19)–(5.32) the state of aggregation of matter was never specified; therefore, the conclusions drawn can be equally applied to solid, liquid, and gaseous media. According to (5.22), (5.27), (5.29), and (5.32), any analysis of shock wave processes must be carried out with the highest consideration for a difference between the thermal effects $Q_{v,T}$, $Q_{p,T}$, and $Q_{p,v}$.

5.4.5 Thermal Criterion for Shock or Detonation

Analysis of expressions (5.13)–(5.15) in comparison with (5.22), (5.27), (5.29), and (5.32) shows that none of the thermal effects $Q_{v,T}$, $Q_{p,T}$, and $Q_{p,v}$ can be regarded as the major thermal characteristic of physicochemical transformation. The variable Q_{cal}, defined in (5.16), is absent in all these expressions. It should be noted that thermal effects (5.13)–(5.16) characterize different aspects of the same transformation $\langle\eta_0\rangle \to \langle\eta\rangle$.

Nevertheless, in shock wave processes the thermal effect $Q_{p,v}$ is of key importance. Let us try to distinguish between the shock and detonation waves by the sign of $Q_{p,v}$ (5.15), which defines the type of physicochemical transformation in a shock.

As shown in [2,64,65,67], the parameters of a detonation wave in condensed and gas-phase explosives are defined by the dynamic adiabat (also termed the "detonation adiabat") that intersects the isochore line v_0 for $p > p_0$. In other words, this dynamic adiabat lies above the point (p_0, v_0) (Fig. 5.9). As a result, the detonation adiabat has a point of contact (Chapman–Jouguet point) with one of the Rayleigh lines, as shown in Fig. 5.9. From [2,64,65,67], the detonation wave corresponding to the Chapman–Jouguet point must obey the condition $D - u = c$ (Fig. 5.8) so that the tail rarefaction waves cannot overtake the shock. Such a shock may be expected to become self-sustaining.

Therefore, the detonation adiabats (and respective detonation waves) in HEs and reactive gaseous mixtures must obey the equivalent inequalities given in (5.3):

Note that inequalities (5.3) characterize a given transformation only at p_0. Nevertheless, these can also be used to predict the features of shock-induced transformation for $p \gg p_0$.

We propose regarding inequalities (5.3) as an intrinsic property of the detonation adiabat and/or the detonation wave in any media, including HEs and reactive gaseous mixtures. For example, inequalities (5.3) are applicable to the so-called condensational shocks in a mixture of air with oversaturated water vapor [2]. Therefore, condensation shocks can also be regarded as detonation waves.

We suggest considering inequalities (5.33) as an intrinsic property of the shock wave:

$$Q_{p,v} \leqslant 0,\ \Delta v_{p,h} \leqslant 0. \tag{5.33}$$

For instance, the dynamic adiabats passing through the point (p_0, v_0) (see Fig. 5.9) and respective shocks without transformations can be classified, according to (5.33), as shock adiabats and shock waves, respectively. In this case, criteria (5.33) are consistent with the accepted opinion.

Applying criteria (5.3) and (5.33), one has to keep in mind that, during physicochemical transformation, the values of $Q_{p,v}$ and $\Delta v_{p,h}$ may change their sign. In the case when criterion (5.3) is not applicable to the final products but is applicable to some intermediate products, one can also expect the onset of detonation in this system.

Criteria (5.3) and (5.33) are not always consistent with the definitions of detonation and shock waves adopted by some workers in the physics of explosions: the detonation wave is regarded as any shock accompanied by exothermic reaction ($Q_{v,T} > 0,\ Q_{p,T} > 0$). But not every reaction that satisfies the inequality $Q_{p,T} > 0$ can satisfy the condition $Q_{p,v} > 0$ (5.3). According to (5.33), some shocks that are accompanied by exothermic reactions can nevertheless be classified only as shock waves.

The Chapman–Jouguet detonation theory [2, 64, 65, 67] acknowledges the existence of a detonation adiabat as a prerequisite for the occurrence of detonation in a given medium. This statement is equivalent to criterion (5.3). This condition is a prerequisite for self-sustaining shock propagation in a given medium.

Therefore, the above analysis of dynamic adiabats suggests that either of the inequalities (5.3) is indeed *a sufficient and necessary thermodynamic condition for the occurrence of detonation* in a given medium.

Note in conclusion that criterion (5.3) is strictly thermodynamic in nature. In other words, the criterion does not define specific conditions for realization of a detonation. These conditions have to be determined by experiment. One such condition is a sufficiently high rate of reaction [3, 64, 67]. Some methods for acceleration of shock-induced reactions were suggested in [27, 68, 69], but none of these methods may help in the initiation of detonation if condition (5.3) is not satisfied, at least for intermediate products. When inequalities (5.3) are not fulfilled (at least for one of the intermediate products), all the dynamic adiabats for a given medium will intersect the isobar $p = p_0$ for $v < v_0$. In this case, the Chapman–Jouguet point does not exist, and hence a self-sustaining shock wave process is impossible.

References

1. Lee, J.H.S., Goroshin, S., Yoshinaka, A., Romano, M., Jiang, J., Hooton, I., Zhang, F.: Attempts to initiate detonations in metal–sulfur mixtures. In: Furnish, M.D., Chhabildas, L.C., Hixton, R.S. (eds.) Shock Compression of Condensed Matter-1999, pp. 775–778. American Institute of Physics, Melville (2000)
2. Landau, L.D., Lifshitz, E.M.: Fluid Mechanics, chaps. 9, 14. Butterworth-Heinemann, Oxford (1987)
3. Kuznetsov, N.M.: Detonation and gas-dynamic jumps during phase transformations in metastable compounds. Zh. Eksp. Teor. Fiz. **49**, 1526–1531 (1965)
4. Merzhanov, A.G., Gordopolov, Yu.A., Trofimov, V.S.: On the possibility of gas-free detonation in condensed systems. Shock Waves **6**, 157–159 (1996)
5. Ryabinin, Yu.N.: Sublimation of a crystal lattice under the action of a strong shock wave. Sov. Phys. Dokl. **1**, 424–426 (1956)
6. Trofimov, V.S.: Dynamic study on relaxation processes. Fiz. Goreniya Vzryva **17**(5), 93–101 (1981)
7. Batsanov, S.S., Doronin, G.S., Koshevoi, V.P., Stupnikov, V.P.: Measurement of the residual temperature of substances after shock compression. Combust. Explos. Shock Waves **4**, 64–66 (1968)
8. Batsanov, S.S., Shestakova, N.A., Stupnikov, V.P., Litvak, G.S., Nigmatullina, V.M.: Shock-induced synthesis of chromium chalcogenides. Proc. Acad. Sci. USSR Dokl. Chem. **185**, 174–175 (1969)
9. Gur'ev, D.L., Batsanov, S.S.: Experimental technique for measurement of post-shock temperature. Bull. Am. Phys. Soc. **30**, 1320–1324 (1985)

10. Gur'ev, D.L., Batsanov, S.S.: Measurement of residual temperatures in cylindrical shock recovery capsules. Combust. Explos. Shock Waves **22**, 490–492 (1986)
11. Batsanov, S.S., Gur'ev, D.L.: Interaction of sulfur with tin in shock waves. Combust. Explos. Shock Waves **23**, 236–237 (1987)
12. Hornig, H., Kury, J., Simpson, R., Helm, F., von Holle, W.: Shock ignition by pyrotechnic heat powder. In: Proceedings XI International Pyrotechnics Seminar, pp. 699–720, Vail (1986)
13. Boslough, M.B.: Shock-induced chemical reactions in nickel–aluminum powder mixtures: radiation pyrometer measurements. Chem. Phys. Lett. **160**, 618–622 (1989)
14. Boslough, M.B.: A thermochemical model for shock-induced reactions (heat detonation) in solids. J. Chem. Phys. **92**, 1839–1848 (1990)
15. Batsanov, S.S., Gogulya, M.F., Brazhnikov, M.A., Lazareva, E.V., Doronin, G.S., Klochkov, S.V., Banshchikova, M.B., Fedorov, A.V., Simakov, G.V.: Shock compression of reactive substances in the system tin–chalcogene. Sov. J. Chem. Phys. **10**, 2635–2638 (1993)
16. Batsanov, S.S., Gogulya, M.F., Brazhnikov, M.A., Simakov, G.V., Maksimov, I.I.: Behavior of the reacting system Sn + S in shock waves. Combust. Explos. Shock Waves **30**, 361–365 (1994)
17. Batsanov, S.S.: Solid-phase reactions in shock waves: kinetic studies and mechanism. Combust. Explos. Shock Waves **32**, 102–113 (1996)
18. Gogulya, M.F., Voskoboinikov, I.M., Dolgoborodov, A.Y., Dorokhov, N.S., Brazhnikov, M.A.: Interaction of sulfur with metals under shock loading. Sov. J. Chem. Phys. **11**, 224–228 (1992)
19. Gogulya, M.F., Brazhnikov, M.A.: On the characteristic times of chemical reactions in heterogeneous systems under dynamic load. Chem. Phys. Rep. **13**, 1887–1890 (1995)
20. Tyte, D. Interaction of metallic powders with a shock wave through an oxidizing atmosphere. J. Appl. Phys. **37**, 802–806 (1966)
21. Batsanov, S.S., Doronin, G.S., Nerchenko, A.A., Roman'kov, V.V., Strelyaev, A.E., Stupnikov, V.P.: Breaking of high-speed flows in different media. J. Eng. Phys. **24**, 354–355 (1973)
22. Kovalenko, A.N., Ivanov, G.V.: Physical and chemical transformations of lead nitrate in mixtures with aluminum under shock waves. Combust. Explos. Shock Waves **17**, 82–85 (1981)
23. Batsanov, S.S., Doronin, G.S., Klochkov, S.V., Teut, A.I.: Synthesis reaction behind shock fronts. Combust. Explos. Shock Waves **22**, 765–769 (1986)
24. Gordopolov, A.Yu., Gordopolov, Y.A., Fedorov, V.M., Shikhverdiev, R.M.: Shock-induced chemical transformations in the Ti–C mixture. In: Proceedings XII Symposium on Combustion and Explosion, part II, pp. 190–192, Chernogolovka (2000)
25. Jiang, J., Goroshin, S., Lee, J.H.S.: Shock wave induced chemical reaction in Mn + S mixture. In: Schmidt, S.C., Dankbar, D.P., Forbes, J.W. (eds.) Shock Compression of Matter–1997, pp. 655–658. Elsevier, New York (1998)
26. Gur'ev, D.L., Gordopolov, Yu.A., Batsanov, S.S.: Solid-state synthesis of ZnTe in shock waves. Combust. Explos. Shock Waves **42**, 116–123 (2006)
27. Xu, X., Thadhani, N.N.: Investigation of shock-induced reaction behavior of as-blended and ball-milled Ni + Ti powder mixtures using time-resolved stress measurements. J. Appl. Phys. **96**, 2000–2009 (2004)

28. Graham, R.A., Anderson, M.U., Horie, Y., Yu, S.-K., Holman, G.K.: Pressure measurements in chemically reacting powder mixtures with the Bauer piezoelectric polymer gauge. Shock Waves **3**, 79–82 (1993)
29. Thadhani, N.N., Graham, R.A., Royal, T., Dunbar, E., Anderson, M.U., Holman, G.K.: Shock-induced chemical reactions in titanium–silicon powder mixtures of different morphologies: time-resolved pressure measurements and materials analysis. J. Appl. Phys. **82**, 1113–1128 (1997)
30. Vandersall, K.V., Thadhani, N.N.: Time-resolved measurements of the shock-compression response of Mo + Si elemental powder mixtures. J. Appl. Phys. **94**, 1575–1583 (2003)
31. Batsanov, S.S., Andrianova, E.E., Lazareva, E.V.: Mechanical consequences of chemical conversions in shock-recovery capsules. Sov. J. Chem. Phys. **9**, 2371–2373 (1991)
32. Batsanov, S.S., Gavrilkin, S.M., Gordopolov, A.Y., Gordopolov, Yu.A.: Spalling phenomena in shock-recovery capsules during shock compression of inert and reactive mixtures. Combust. Explos. Shock Waves **40**, 605–611 (2005)
33. Batsanov, S.S., Lazareva, E.V., Kopaneva, L.I.: Shock wave interaction of metals with water. High Energy Chem. **16**, 150–150 (1982)
34. Batsanov, S.S., Lazareva, E.V., Kopaneva, L.I.: Interaction of metals and water under dynamic compression. Sov. J. Chem. Phys. **3**, 1403–1403 (1985)
35. Batsanov, S.S., Gur'ev, D.L., Kopaneva, L.I.: Shock synthesis of the cubic ZrO_2. Combust. Explos. Shock Waves **24**, 505–505 (1988)
36. Sekine, T.: Diamond from shocked magnesite. Naturwissenschaften **75**, 462–463 (1988)
37. Batsanov, S.S., Blokhina, G.E., Deribas, A.A.: The effect of explosion on materials: structural changes in boron nitride. J. Struct. Chem. **6**, 209–213 (1965)
38. Akashi, T., Sawaoka, A., Saito, S., Araki, M.: Structural changes of boron nitride caused by multiple shock-compression. Jpn. J. Appl. Phys. **15**, 891–892 (1976)
39. Sokolowski, M.: Deposition of wurtzite-type boron nitride layers by reactive plus plasma crystallization. J. Cryst. Growth **46**, 136–138 (1979)
40. Fedoseev, D.V., Varshavskaya, I.G., Lavrent'ev, A.V., Deryagin, B.V.: Phase transformations of small-size solid particles during laser heating. Dokl. Phys. Chem. **270**, 416–418 (1983)
41. Sokolowska, A., Wronikowski, M.: The phase diagram (P, T, E) of boron nitride. J. Cryst. Growth **76**, 511–513 (1986)
42. Akashi, T., Pak, H.-R., Sawaoka, A.: Structural changes of wurtzite-type and zinc blend-type boron nitride by shock treatment. J. Mater. Sci. **21**, 4060–4066 (1986)
43. Nameki, H., Sekine, T., Kobayashi, T., Fat'yanov, O.V., Sato, T., Tashiro, S.: Rapid quench formation of E-BN from shocked turbostratic BN precursors. J. Mater. Sci. Lett. **15**, 1492–1494 (1996)
44. Gagnier, M., Szwarc, H., Ronez, A., Low-energy ball-milling: Transformations of boron nitride powders. Crystallographic and chemical characterizations. J. Mater. Sci. **35**, 3003–3009 (2000)
45. Batsanov, S.S.: The E-phase of boron nitride as a fullerene. Combust. Explos. Shock Waves **34**, 106–108 (1998)
46. Batsanov, S.S., Kopaneva, L.I., Lazareva, E.V., Kulikova, I.M., Barinsky, R.L.: On the nature of boron nitride E-phase. Propellants Explos. Pyrotech. **18**, 352–355 (1993)

47. Batsanov, S.S., Deribas, A.A.: The effect of explosion on materials: structural changes in neodymium oxide. Combust. Explos. Shock Waves **1**, 77–79 (1965)
48. Batsanov, S.S., Kopaneva, L.I., Lazareva, E.V., Gavryushin, V.N., Isaev, V.N., Porokhov, P.V.: Formation of the $Zr_{1-x}Fe_xS_2$ solid solution as a result of microspalling at shock compression in recovery ampoules. Combust. Explos. Shock Waves **26**, 614–615 (1990)
49. Kikuchi, M., Syono, Y., Fukuoka, K., Hiraga, K.: Redox reaction between tantalum and silica induced by shock loading. J. Mater. Sci. Lett. **6**, 97–99 (1987)
50. Batsanov, S.S., Shevtsova, N.N., Temnitskii, I.N., Bokarev, V.P.: Thermal and shock-induced synthesis of hybride germanium chalcogenides. Russ. J. Inorg. Chem. **31**, 925–926 (1986)
51. Shevtsova, N.N., Temnitskii, I.N., Batsanov, S.S.: The impact synthesis of the α- and β-forms of GeSeTe. Russ. J. Inorg. Chem. **32**, 1512–1513 (1987)
52. Batsanov, S.S., Bokarev, V.P., Maksimov, I.I., Tumanov, V.A.: Formation of foams upon dynamic/static compression of powdered dioxides of silicium, germanium and tin. Combust. Explos. Shock Waves **29**, 652–652 (1993)
53. Batsanov, S.S.: Specific features of solid-phase reactions induced by shock waves. Combust. Explos. Shock Waves **42**, 237–241 (2006)
54. Batsanov, S.S.: Inorganic chemistry of high dynamic pressures. Russ. Chem. Rev. **55**, 297–315 (1986)
55. Kostyukov, N.A.: Structure of the flow of binary mixtures of solids at two-dimensional shock wave loading. J. Appl. Mech. Tech. Phys. **29**, 362–365 (1988)
56. Batsanov, S.S., Maksimov, I.I.: Forced diffusion in condensed matter at shock compression. Sov. J. Chem. Phys. **8**, 2156–2157 (1991)
57. Dolgoborodov, A.Yu., Voskoboinikov, I.M., Tolstov, I.K., Sudarikov, A.V.: Characteristic properties of shock wave propagation in mixtures. Combust. Explos. Shock Waves **28**, 308–312 (1992)
58. Horie, Y., Mass mixing and nucleation and growth of chemical reactions in shock compression of powder mixtures. In: Murr, L.E., Staudhammer, K.P., Meyers, M.A. (eds.) Metallurgical and Materials Applications of Shock Wave and High-Strain-Rate Phenomena, pp. 603–614. Elsevier, New York (1995)
59. Batsanov, S.S.: Synthesis and modification of materials by shock waves: Real-time measurements and mechanism of reaction. Mater. Sci. Eng. A **210**, 57–63 (1996)
60. Coustal, R., Prevet, F.: Sur un noveau procédé de preparation du sulfure de zinc phosphorescent. C. R. Acad. Sci. **188**, 703–706 (1929)
61. Torunov, S.I., Trofimov, V.S., Calculation of an equilibrium temperature in ideal detonation wave in the zinc–sulfur SHS system. Int. J. SHS **10**, 13–21 (2001)
62. Torunov, S.I., Trofimov, V.S.: Two possible structures of detonation wave in the Zn–S mixture. In: Abstracts XII Symposium on Combustion and Explosion, part II, pp. 165–166, Chernogolovka (2000)
63. Gur'ev, D.L., Gordopolov, Yu.A., Batsanov, S.S., Fortov, V.E.: Solid-state detonation in the zinc–sulfur system. Appl. Phys. Lett. **88**, 024102 (2006)
64. Johansson, C.H., Persson, P.A.: Detonics of High Explosives. Vinterviken, Stockholm (1970)
65. Cook, M.A.: The Science of High Explosives. Reinhold, New York (1958)
66. L.D. Landau, E.M. Lifshits: Statistical Physics, chap. 1. Butterworth-Heinemann, Oxford (1980)

67. Dremin, A.N., Savrov, S.D., Trofimov, V.S., Shvedov, K.K.: Detonatsionnye Volny v Kondensirovannykh Sredakh (Detonation Waves in Condensed Matter), p. 20. Nauka, Moscow (1970)
68. Dolgoborodov, A.Yu., Makhov, M.N., Kolbanev, M.N., Streletskii, A.N., Fortov, V.E.: Detonation in an aluminum-teflon mixture, JETP Lett. **81**, 311–314 (2005)
69. Dolgoborodov, A.Yu., Makhov, M.N., Kolbanev, M.N., Streletskii, A.N., Fortov, V.E.: Detonation in metal-teflon mechanoactivated composites. In: Proc. XIV International Detonation Symposium, Norfolk (2006)